Metallography, Microstructure, and Analysis (2024) 13:106–113
https://doi.org/10.1007/s13632-023-01031-4

ORIGINAL RESEARCH ARTICLE

Significant Texture Weakening of AZ91 Alloy by Asymmetric Hot Rolling

Ebrahim Tolouie[1] · **Roohollah Jamaati**[1]

Received: 1 August 2023 / Revised: 2 November 2023 / Accepted: 19 November 2023 / Published online: 14 December 2023

Abstract

The asymmetric hot rolling was applied to the as-cast AZ91 alloy to weaken the texture. It was found that the {0001} basal slip was not favored during deformation due to the presence of a strong ⟨0001⟩ orientation in the as-cast sample. Surprisingly, the fraction of contraction twins was much larger than extension ones owing to the high content of $Mg_{17}Al_{12}$ intermetallic compounds. The incoherent $Mg_{17}Al_{12}$ at the grain boundaries could limit and/or prevent the nucleation of the thick extension twin, but did not hinder the narrower twin (contraction and double) nucleation. A large amount of β phase within α grains provided more possibilities to reduce twin boundary migration, and thus, the growth of thick extension twins was hindered. The presence of the $Mg_{17}Al_{12}$ phase in the starting material was responsible for changing the twinning process. The asymmetric hot rolling led to significant texture weakening in the AZ91 alloy.

Keywords Texture · Magnesium alloy · Asymmetric hot rolling

Introduction

Magnesium and its alloys as very light metals can be used in aerospace and transportation industries [1–3]. However, magnesium and its alloys exhibit poor deformation capability and strong anisotropy at ambient temperature due to their limited slip systems available and the strong basal texture formed [4, 5]. These are big challenges in the studies and applications of magnesium alloys. To improve the ductility of magnesium and its alloys, two approaches have been performed: grain refinement and texture modification through dynamic recrystallization [1, 4–10] and the addition of alloying elements [2, 3, 11].

Guan et al. [6, 12] studied the individual impact of recrystallization on the weakening of texture in a magnesium alloy. Their results showed that double twins and shear bands decrease the intensity of deformation texture (i.e., {0002} fiber texture). Su et al. [13] studied the relationship between texture weakening and recrystallization in the AZ31 sheets processed by rolling. Weakening of texture was achieved after annealing owing to the occurrence of recrystallization on shear bands and twins. This remarkably enhanced ductility. Ding et al. [14] reported a weakening of texture and improvement of ductility in a Mg–2Zn alloy by the addition of Ca or RE. They found that the addition of zinc to pure magnesium leads to the formation of basal texture, while the addition of zinc to magnesium–calcium alloy results in a spread of basal poles toward the transverse direction and a reduction in texture intensity.

Recently, to obtain high strength and good ductility in the AZ91 alloy, several techniques have been used. Ghandehari Ferdowsi et al. [15] report the impact of the high-temperature rolling process and annealing on the microstructural evolution and texture of the homogenized AZ91. They showed that a basal texture with high intensity was first generated. By performing annealing, the intensity of basal texture decreased. Alili et al. [16] investigated the texture of AZ91 after high-temperature rolling and subsequent annealing treatment. After the rolling process at 400 °C, a basal deformation texture with the splitting of the basal poles was formed. After long-term annealing treatment, the basal texture has remained. Wang et al. [17] investigated the microstructure and mechanical behavior of AZ91 rolled from three different initial conditions consisting of as-cast, as-extruded, and cast-rolling. The microstructure of all samples exhibited

✉ Roohollah Jamaati
jamaati@nit.ac.ir

[1] Department of Materials Engineering, Babol Noshirvani University of Technology, Shariati Ave., Babol 47148–71167, Iran

fine grains and a high-density basal texture in all three samples was formed.

Based on the aforementioned results, it is difficult to obtain a very weak {0002} basal texture in the AZ91 alloy. Asymmetric rolling as a plastic deformation technique changes the microstructure and texture compared to conventional rolling. In asymmetric rolling, the speed of the lower and upper rolls is different. Therefore, intense shear plastic deformation can be produced throughout the sheet thickness, which changes the texture from basal to other orientations. It is important to explore the capability of the asymmetric hot rolling process to weaken the basal texture of AZ91. Therefore, the current work aims to study the influence of the asymmetric hot rolling process on the microstructure and texture evolution of as-cast AZ91 without homogenization or annealing treatments.

Experimental Procedure

The raw material used in this work was as-cast AZ91 (Mg–8.4Al–1.3Zn–0.3Mn) alloy. Before rolling deformation, the as-cast AZ91 was machined into sheet-type samples with dimensions of $70 \times 20 \times 3.5$ mm^3. The sheets were preheated at 400 °C for 600 s and asymmetrically rolled with two total deformations of 8% and 15%. The method of asymmetric rolling in the present work was single-roll drive rolling. The asymmetric rolling was performed on a laboratory rolling mill with 150 mm and the rotational speed of the driven (lower) roller was fixed at 2 rpm. The upper roller was idle.

Microstructural characterization was performed by optical microscopy (OM). The samples were sectioned from the ND (normal direction) plane and the center of the sheet. The samples were ground with SiC papers, polished with alumina suspension, and finally etched with picral reagent. Macrotexture was evaluated by X-ray diffraction (XRD) with Cu Kα radiation. The orientation distribution functions (ODFs) and pole figures (PFs) were obtained by the TexTools software.

Results

Optical micrographs of as-cast and deformed AZ91 are shown in Fig. 1. The microstructure of the as-cast material mainly comprises α-Mg grains, β-$Mg_{17}Al_{12}$ intermetallics (located at the grain boundaries (continuous type) and in the interior of the grains (discontinuous type)), $\alpha+\beta$ eutectic phase (adjacent to the $Mg_{17}Al_{12}$ phase), and Al_8Mn_5 particles. It should be noted no twins are observed in the as-cast AZ91 sample. The average grain size of the alpha phase is 62 µm. After 8% asymmetric hot rolling, as shown in Fig. 1b, the volume fraction of the β-$Mg_{17}Al_{12}$ reduced owing to the dissolution of the β in the α-Mg grains. Also, the average grain size of the α-Mg slightly increased. In addition, many $\left\{10\bar{1}1\right\}$ or $\left\{10\bar{1}3\right\}$ contraction (compression) twins (CTs) with thin and extended morphology formed in the AZ91 alloy, and $\left\{10\bar{1}2\right\}$ extension (tension) twins (ETs) with thick and lenticular shapes were nearly absent, as shown in Fig. 1b. Moreover, some cross-twins exist in the microstructure after 8% deformation. Looking at the optical micrograph of Fig. 1c, no remarkable change is observed in the average grain size by even 15% hot rolling of the AZ91 alloy. Compared with the previous sample (Fig. 1b), the 15% hot-rolled sample contains a much higher density of contraction (and maybe $\left\{10\bar{1}1\right\}-\left\{10\bar{1}2\right\}$ double) twins and also twin intersections. Some extension twins are formed in the microstructure of the sample after 15% strain. With regard to Fig. 1b, c, there is no sign of dynamic recrystallization (DRX) mechanisms during hot rolling of AZ91 alloy up to 15% thickness reduction.

The distribution of misorientation angle for as-cast and deformed samples are depicted in Fig. 2. Also, the volume fraction of low-angle boundaries (LABs) with $\theta<15°$, high-angle boundaries (HABs) with $15°<\theta<65°$, and extra high-angle boundaries (EHABs) with $\theta>65°$ in all samples is plotted in Fig. 3. As illustrated in Figs. 2 and 3, the fraction of grains with LABs after 0, 8, and 15% deformation are 1.6, 1.3, and 1.3%, respectively. In contrast, the fraction of grains with HABs gradually increased from 51.7% (for the as-cast sample) to 54.4% (after 15% strain). In addition, the fraction of grains with EHABs gradually reduced from 46.6% (before hot rolling) to 44.5% (for the 15% deformed sample). Based on the non-occurrence of recrystallization in the microstructure of AZ91 alloy (see Fig. 1), it can be stated that the variations of misorientation during rolling are attributed to the rotation of preexisting grains (owing to slip) and formation of mechanical twins (contraction, extension, and double). It should be noted that the misorientation of {0002} at the twin boundaries is 86.3°, 56.2°, and 37.5° for $\left\{10\bar{1}2\right\}$ extension, $\left\{10\bar{1}1\right\}$ contraction, and $\left\{10\bar{1}1\right\}-\left\{10\bar{1}2\right\}$ double twins, respectively [1, 6, 11, 12]. In fact, the contraction and double twins have HABs, while the extension twin boundaries are EHAB. With regard to Figs. 1 and 3, it can be concluded that the extensive contraction and perhaps double twinning are responsible for increasing the volume fraction of HAB.

Figures 4 and 5 depict the {0002} PFs and ODFs of AZ91 alloy under different deformations, respectively. From Fig. 4a, the texture of the as-cast sample is mainly characterized by a strong $\langle 0001 \rangle$ texture. Figure 5a indicates that two texture components, i.e., $\left(01\bar{1}0\right)\left[2\bar{1}\bar{1}6\right]$ and

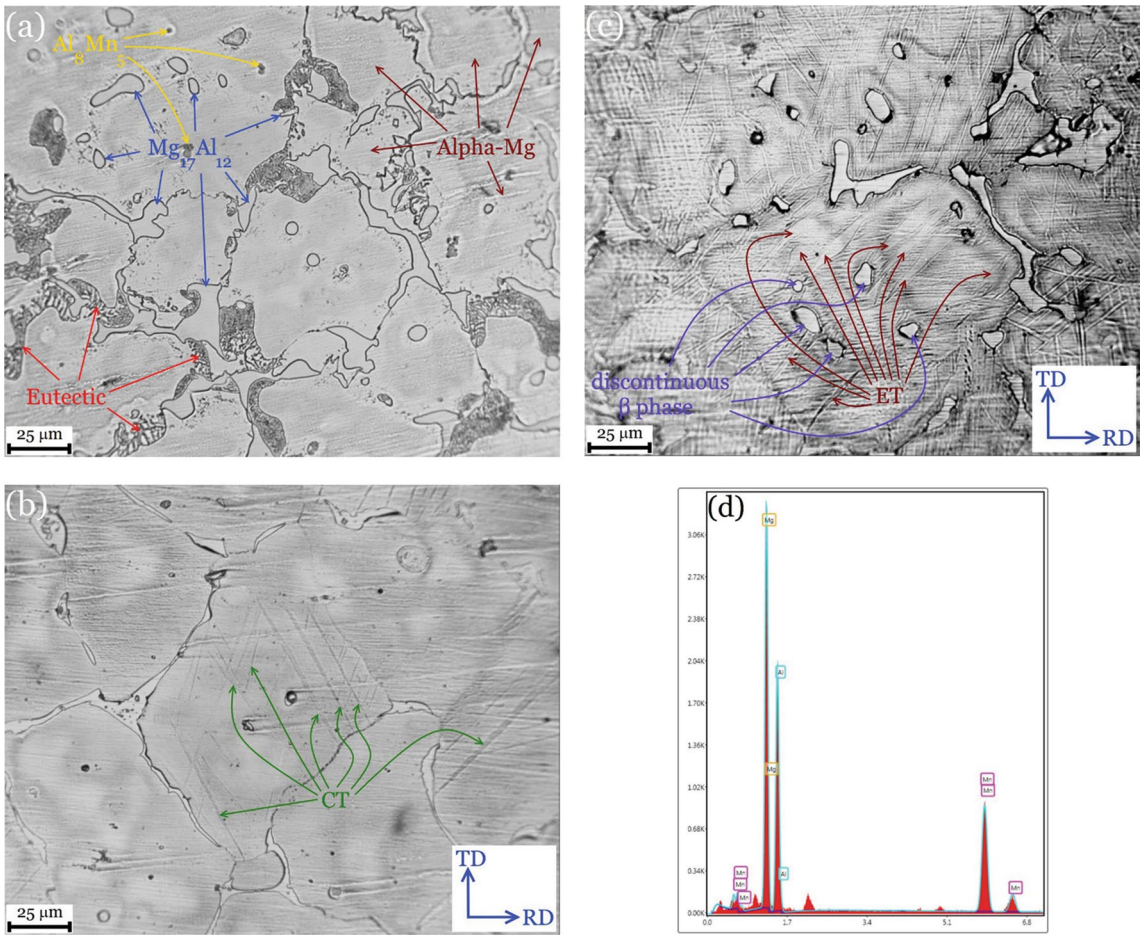

Fig. 1 Microstructures of (**a**) 0% (as-cast), (**b**) 8%, and (**c**) 15% hot-rolled AZ91. (**d**) EDS analysis of the Al_8Mn_5 particles

$\left(01\bar{1}0\right)[0001]$, with intensity of 116.6×R and 62.3×R, respectively, are dominant for the as-cast AZ91. After an 8% rolling reduction, the intensity of ⟨0001⟩||RD decreases and some grains rotate toward the basal pole (center of PF). The main orientations for this sample are $\left(01\bar{1}0\right)\left[2\bar{1}\bar{1}6\right]$, $\left(11\bar{2}2\right)\left[10\bar{8}\bar{2}3\right]$, $\left(11\bar{2}4\right)\left[1\bar{1}00\right]$, $\left(11\bar{2}3\right)\left[7\bar{5}\bar{2}3\right]$, $\left(01\bar{1}0\right)\left[2\bar{1}\bar{1}6\right]$, $\left(11\bar{2}3\right)\left[2\bar{1}\bar{1}\bar{1}\right]$, and $\left(01\bar{1}0\right)[0001]$ with the intensity of 36.5×R, 22.5×R, 22×R, 21.2×R, 20.9×R, 10.1×R, and 3.2×R, respectively. Finally, for the 15% deformed sample, the ⟨0001⟩||RD weakens again and more grains rotate to the basal pole. As shown in Fig. 5c, there are multiple texture components including $\left(01\bar{1}0\right)\left[2\bar{1}\bar{1}6\right]$, $\left(01\bar{1}0\right)[0001]$, $(0001)\left[5\bar{4}\bar{1}0\right]$, $\left(11\bar{2}3\right)\left[1\bar{1}00\right]$, $(0001)\left[13\bar{4}\bar{1}\right]$, $\left(11\bar{2}3\right)\left[2\bar{1}\bar{1}\bar{1}\right]$, $(0001)\left[2\bar{1}\bar{1}0\right]\left(11\bar{2}2\right)\left[1\bar{1}00\right]$ $\left(11\bar{2}6\right)\left[5\bar{3}\bar{2}1\right]\left(01\bar{1}7\right)\left[2\bar{1}\bar{1}0\right]\left(01\bar{1}3\right)\left[30\bar{3}1\right]\left(11\bar{2}4\right)\left[5\bar{1}\bar{4}3\right]$ $\left(11\bar{2}5\right)\left[8\bar{4}\bar{4}3\right]$ with the intensity of 14.2×R, 6×R, 5.7×R, 5.2×R, 4.9×R, 4.7×R, 4.6×R, 4.5×R, 4.5×R, 3.9×R, 3.8×R, 3.8×R, and 3.7×R, respectively. With regard to PFs and ODFs, the overall texture intensity significantly decreased by asymmetric hot rolling up to 15% strain.

Discussion

Initial orientation has an important effect on the activation of deformation mechanisms such as slip and twinning. Figures 4a and 5a indicate that there is a strong ⟨0001⟩||RD orientation in the as-cast sample. In other words, the c-axis of many α-Mg grains is approximately parallel to the rolling direction. In this type of texture, the Schmid factor is very low or even zero. Consequently, no resolved shear stress is applied on the {0002} and the dislocation slip is hindered under both compression and tension stresses. The rolling

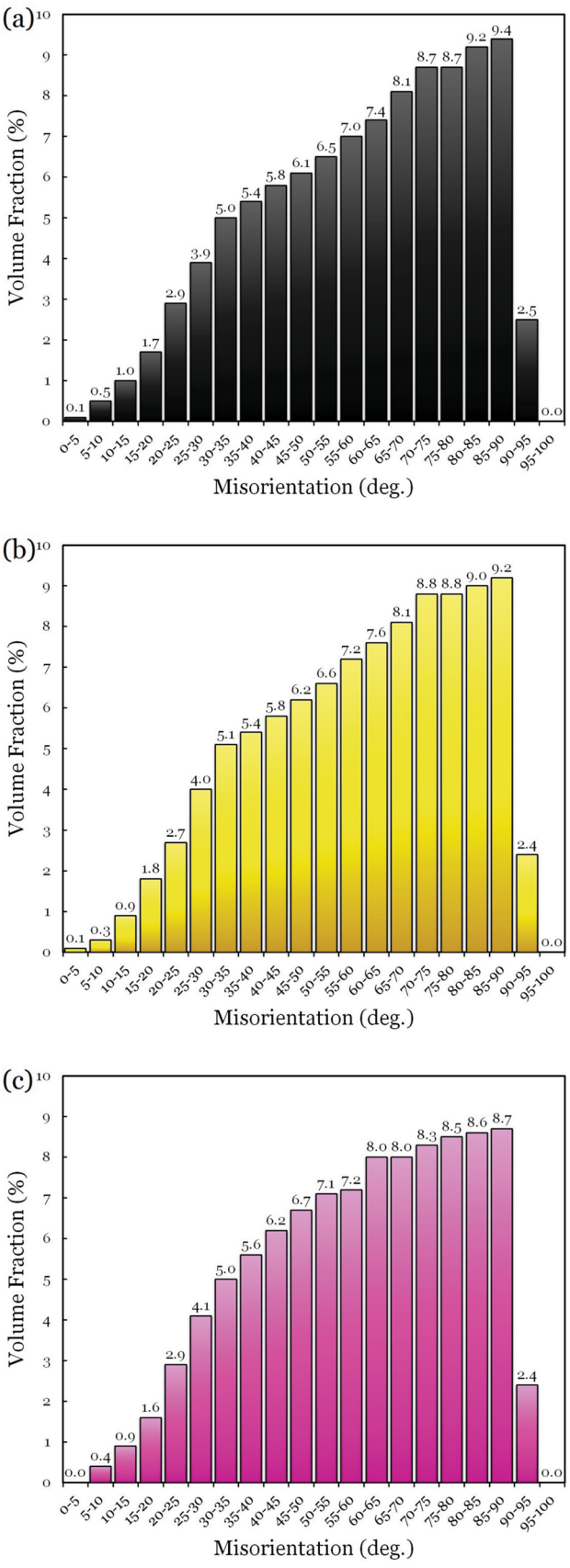

Fig. 2 Misorientation distributions of (**a**) 0% (as-cast), (**b**) 8%, and (**c**) 15% hot-rolled AZ91

process can be considered as subjecting tension in the rolling direction and compression in the normal direction. Therefore, the {0001} basal slip is not favored during the rolling deformation of as-cast AZ91. When the basal slip becomes difficult or completely suppressed due to ⟨0001⟩||RD texture, then the AZ91 alloy would deform by prismatic and/or pyramidal slip systems. However, in this condition, the mechanical twinning is prominent over prismatic and pyramidal slips. The only reason why prismatic and pyramidal slips are not dominant is that the critical resolved shear stress (CRSS) of twinning is much lower than that of pyramidal and prismatic slips [18, 19]. As shown in Fig. 1, the volume fraction of twins increased after a 15% thickness reduction because the stress for activation of twinning remains smaller than that of pyramidal and/or prismatic slip systems.

There are three types of mechanical twinning in magnesium alloys including $\left\{10\bar{1}2\right\}$ extension, $\left\{10\bar{1}1\right\}$ or $\left\{10\bar{1}3\right\}$ contraction, and $\left\{10\bar{1}1\right\}-\left\{10\bar{1}2\right\}$ double twinning, in the order of increasing difficulty in activation [20–22]. The CRSS value of extension twins is less than 5 MPa, which is much lower than the CRSS of contraction twins (between 30 and 100 MPa). The low CRSS value of extension twins makes its operation possible even at a low level of stress and a low temperature. It was reported that the volume fraction of extension twins quickly enhances with deformation, reaching more than 80% at a deformation of 8% [23, 24]. On the other hand, activation of a contraction twin is difficult owing to its larger critical resolved shear stress value, and the activation of double twins is more difficult since they have to originate within contraction twin interiors [22]. However, as shown in Figs. 1b, c, the fraction of contraction twins was much higher than extension twins. This is a very surprising finding. This can be attributed to the high content of $Mg_{17}Al_{12}$ intermetallic compounds at the grain boundaries.

Unlike the slip, the twinning involves nucleation and growth, and the second phase particles will influence both processes. Grain boundaries are the potential sites for the nucleation of twins in magnesium [25–27], and therefore, any changes in the structure of grain boundaries affect twin nucleation. It should be noted that in most works on the AZ series magnesium alloys, a homogenized structure was used as the starting material [4, 8–10, 13, 15–17, 19, 20, 24, 27]. But, in the present work, we used the as-cast structure without homogenization treatment. Therefore, it can be said that the presence of a high amount of discontinuous and continuous particles at the grain boundaries can significantly change potential twin nucleation

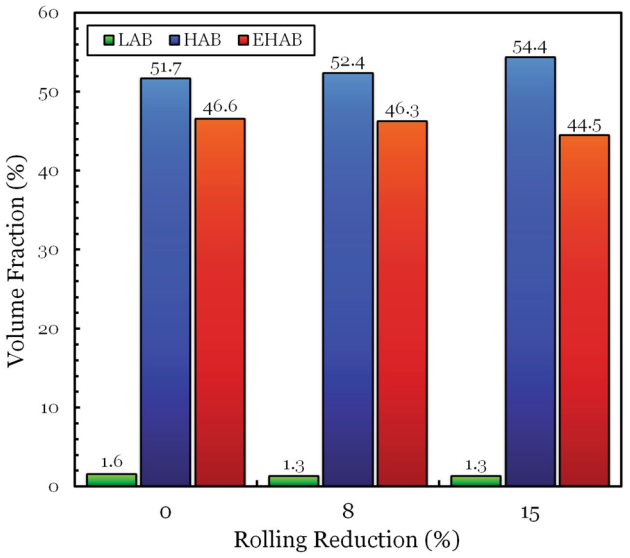

Fig. 3 Volume fraction of LAB, HAB, and EHAB for (**a**) 0% (as-cast), (**b**) 8%, and (**c**) 15% hot-rolled AZ91

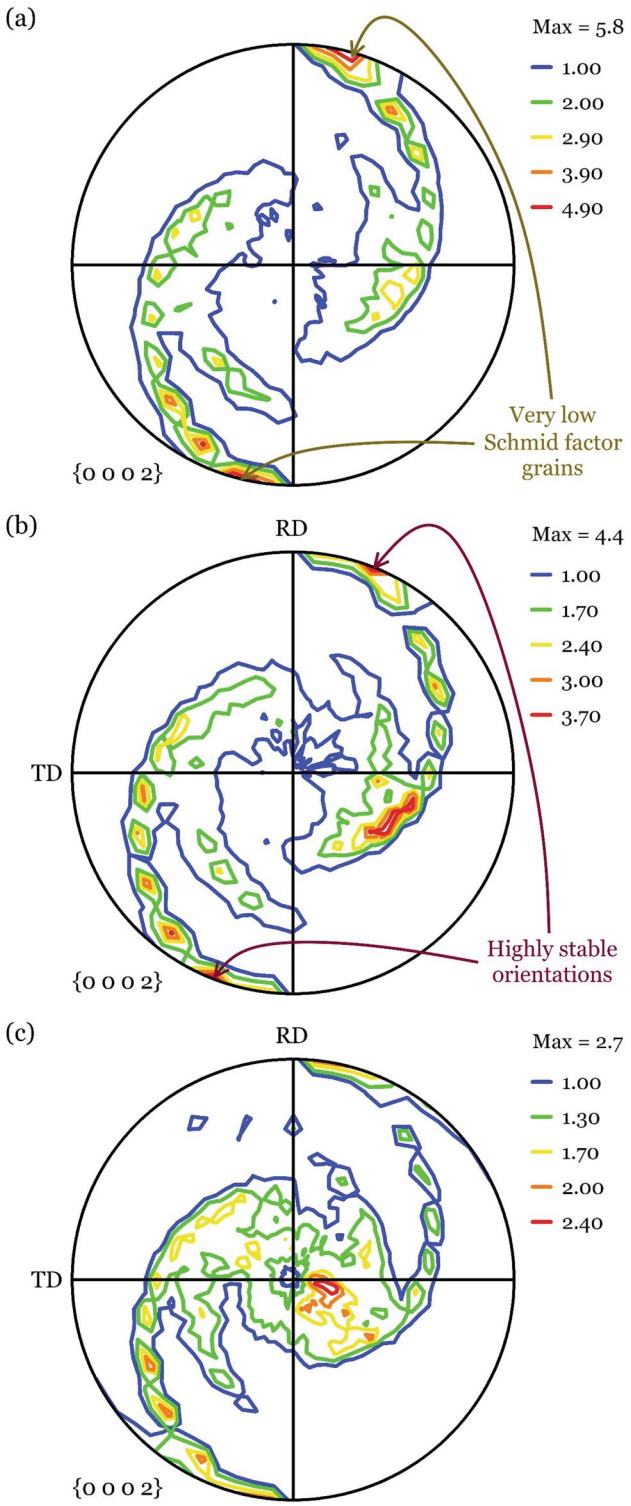

Fig. 4 Pole figures of (**a**) 0% (as-cast), (**b**) 8%, and (**c**) 15% hot-rolled AZ91

sites. Beyerlein et al. [28] reported that the nucleation of twins is attributed to the misorientation of the boundaries. The extension twins connected to boundary segments with smaller (<45°) misorientation are more than those with larger misorientation. In fact, by increasing the coherency of the boundaries, the chance for the nucleation of twins is enhanced. Thus, it can be stated that the incoherent $Mg_{17}Al_{12}$ intermetallic compounds at the grain boundaries can limit and/or prevent the thick twin (extension twin) nucleation, but do not inhibit the nucleation of narrow twin (contraction and double twins). In addition, extension twins generally nucleate at the grain boundaries, then rapidly propagate within the grain, and finally terminate at the next grain boundary. The extension twin termination creates a stress concentration leading to the stimulation of the twin nucleation in the next grain [29–31]. Therefore, the large amount of continuous $Mg_{17}Al_{12}$ intermetallic compounds can hinder the twin nucleation in the neighboring grain.

With regard to Fig. 1c, during 15% hot rolling, a few extension twins formed, but the growth of these twins was limited. After the nucleation of twins, the growth depends on various dislocation glide mechanisms [14, 17–19]. Therefore, the lengthening and widening of nucleated twins are mainly related to the twin boundary migration. The twin boundary mobility decreases by three factors consisting of loss of coherency [32], high amount of solute atoms within grains [33], and presence of second phase particles [34]. In the present work, the alpha grains in AZ91 alloy have a low amount of aluminum atoms because the homogenization treatment was not performed. On the other hand, from Fig. 1c, there was a large amount of discontinuous β phase within α grains (as indicated by blue arrows). In a particle-free grain, the $\left\{10\bar{1}2\right\}$ twins easily grow and consume the

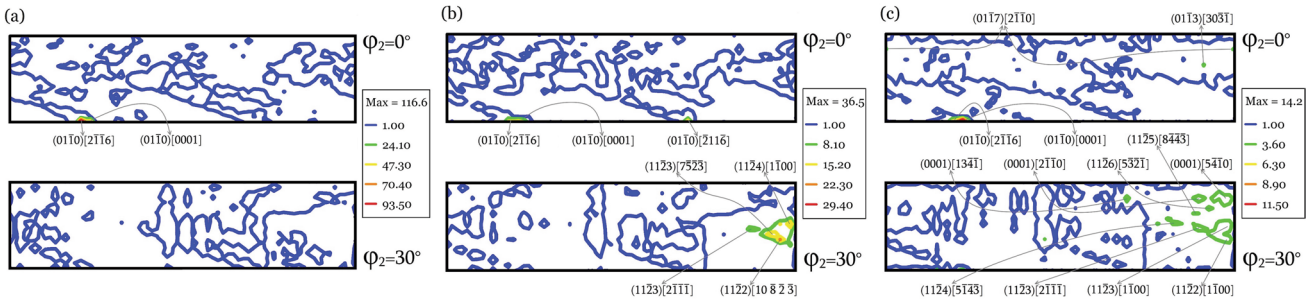

Fig. 5 ODFs of (**a**) 0% (as-cast), (**b**) 8%, and (**c**) 15% hot-rolled AZ91

entire grain. However, the presence of obstacles (i.e., discontinuous $Mg_{17}Al_{12}$ particles) in the path of migrating twin boundaries markedly influences the behavior of twinning in the AZ91. The high discontinuous β phase content within α grains in the present study provided more possibilities to reduce twin boundary migration, and thus, the growth of thick extension twins is inhibited.

Another interesting finding was significant texture weakening during the hot rolling of AZ91 alloy (see Figs. 4 and 5). As shown in Figs. 4a and 5a, most of the grains of the as-cast material were aligned in such a way that the {0002} lie perpendicular to the RD ($\langle 0001 \rangle \| RD$). As mentioned before, these grains have a very low Schmid factor and thus have a highly stable orientation (as indicated in Fig. 4). This texture is not easily transformed to the well-known texture of magnesium alloys (i.e., $\langle 0001 \rangle \| ND$) during rolling deformation. Therefore, the unusual texture evolution in the current research obviously demonstrates that the presence of primary $\langle 0001 \rangle \| RD$ texture can lead to texture weakening in the AZ91 alloy. However, some researchers [32, 35, 36] reported that in a starting structure similar to the present study, a dramatic texture change of about a 90° rotation (i.e., a strong basal texture) and texture strengthening is observed at low strains of 5%. They expressed that the grains with $\langle 0001 \rangle \| RD$ texture have suitable orientation for extension twinning. During deformation, the formation of a large number of extension twins rotates the basal planes of grains with $\langle 0001 \rangle \| RD$ orientation for 86.3° about the $\left\langle 11\bar{2}0 \right\rangle$ crystal directions, resulting in the generation of a strong {0002} basal texture and also texture strengthening. In fact, for magnesium alloys, $\left\{ 10\bar{1}2 \right\}$ twinning plays a decisive role in the formation of a very strong $\langle 0001 \rangle \| ND$ orientation because it gives rise to a lattice rotation of 86.3° [19, 23, 24, 37, 38]. Interestingly, our experimental results are inconsistent with those found in the abovementioned papers. The reason can be attributed to the presence of a large amount of continuous $Mg_{17}Al_{12}$ intermetallic compounds in the as-cast structure as starting material in the present work, which led to a suppression of extension twinning nucleation and stimulation of contraction and/or double twinning. Contraction and double twins reorient the lattice by a 56.2° and 37.5°, respectively, rotation about the $\left\langle 11\bar{2}0 \right\rangle$ directions. Consequently, the contraction and double twins do not remarkably affect the texture during rolling. Based on these findings, therefore, it can be concluded that the change in the twinning process caused by the presence of the β phase in the starting material can remarkably affect the texture evolution.

The asymmetric mode of hot rolling also can be responsible for significant texture weakening after 15% deformation. According to studies by Gong et al. [39, 40], Lou et al. [41], and Chang et al. [42], the texture weakening may be related to severe shear plastic deformation throughout the thickness of the sheet by asymmetric rolling, which enhances the formation of more $\left\{ 10\bar{1}1 \right\} - \left\{ 10\bar{1}2 \right\}$ double twins. On the other hand, during asymmetric hot rolling, prismatic $\langle a \rangle$ slip becomes more easily activated due to intense shear deformation. As a result, texture weakening was observed in the AZ91 alloy processed by asymmetric rolling.

Conclusions

In this study, the influence of asymmetric hot rolling on the microstructure and texture evolution of as-cast AZ91 was evaluated. Microstructure and texture were examined. The following conclusions can be drawn from the current research:

1. The {0001} basal slip was not favored during deformation due to the presence of a strong $\langle 0001 \rangle \| RD$ orientation in the as-cast AZ91.
2. Surprisingly, the fraction of contraction twins in the 15% hot-rolled sample was much larger than extension ones owing to the high content of $Mg_{17}Al_{12}$ intermetallic compounds at the grain boundaries.
3. The presence of incoherent $Mg_{17}Al_{12}$ intermetallic compounds at the grain boundaries can limit and/or prevent

the nucleation of thick extension twins, but does not inhibit the nucleation of narrower (contraction and double) twins.

4. A large amount of β phase within α grains provided more possibilities to reduce twin boundary migration, and thus, the growth of thick extension twins was inhibited.
5. Change of the twinning process caused by the existence of the $Mg_{17}Al_{12}$ phase in the starting material and using the asymmetric mode of hot rolling led to significant texture weakening in the AZ91 alloy.

References

1. S. Biswas, D. Satyaveer Singh, B. Beausir, L. Toth, S. Suwas, Thermal response on the microstructure and texture of ECAP and cold-rolled pure magnesium. Metall. Mater. Trans. A. **46**, 2598–2613 (2015)
2. S. Yu, C. Liu, Y. Gao, S. Jiang, Z. Bao, Dynamic recrystallization mechanism of Mg–8.5Gd–2.5Y–0.4Zr alloy during hot ring rolling. Mater Charact. **131**, 135–139 (2017)
3. C. Fang, G. Liu, X. Liu, H. Hao, X. Zhang, Significant texture weakening of Mg–8Gd–5Y–2Zn alloy by Al addition. Mater. Sci. Eng. A. **701**, 314–318 (2017)
4. S.V.S.N. Murty, N. Nayan, R. Madhavan, S.C. Sharma, K.M. George, S. Suwas, Analysis of microstructure and texture evolution in Mg–3Al–1Zn alloy processed through groove rolling. J. Mater. Eng. Perform. **24**, 2091–2098 (2015)
5. W.J. Kim, H.G. Jeong, H.T. Jeong, Achieving high strength and high ductility in magnesium alloys using severe plastic deformation combined with low-temperature aging. Scripta Mater. **61**, 1040–1043 (2009)
6. D. Guan, W. Mark Rainforth, J. Gao, L. Ma, B. Wynne, Individual effect of recrystallisation nucleation sites on texture weakening in a magnesium alloy: part 2- shear bands. Acta Mater. **145**, 399–412 (2018)
7. H. Zhang, W. Jin, J. Fan, W. Cheng, H.J. Roven, B. Xu, H. Dong, Grain refining and improving mechanical properties of a warm rolled AZ31 alloy plate. Mater. Lett. **135**, 31–34 (2014)
8. X. Huang, K. Suzuki, Y. Chino, Annealing behaviour of Mg–3Al–1Zn alloy sheet obtained by a combination of high-temperature rolling and subsequent warm rolling. J. Alloy. Compd. **509**, 4854–4860 (2011)
9. F. Pilehva, A. Zarei-Hanzaki, S.M. Fatemi-Varzaneh, The influence of initial microstructure and temperature on the deformation behavior of AZ91 magnesium alloy. Mater. Des. **42**, 411–417 (2012)
10. S. Biswas, H.G. Brokmeier, J.J. Fundenberger, S. Suwas, Role of deformation temperature on the evolution and heterogeneity of texture during equal channel angular pressing of magnesium. Mater Charact. **102**, 98–102 (2015)
11. W.J. Ai, G. Fang, J. Zhou, M.A. Leeflang, J. Duszczyk, Effect of twinning on the deformation behavior of an extruded Mg–Zn–Zr alloy during hot compression testing. Mater. Sci. Eng. A. **556**, 373–381 (2012)
12. D. Guan, W. Mark Rainforth, J. Gao, J. Sharp, B. Wynne, L. Ma, Individual effect of recrystallisation nucleation sites on texture weakening in a magnesium alloy: part 1- double twins. Acta Mater. **135**, 14–24 (2017)
13. J. Su, A.S.H. Kabir, M. Sanjari, S. Yue, Correlation of static recrystallization and texture weakening of AZ31 magnesium alloy sheets subjected to high speed rolling. Mater. Sci. Eng. A. **674**, 343–360 (2016)
14. H. Ding, X. Shi, Y. Wang, G. Cheng, S. Kamado, Texture weakening and ductility variation of Mg–2Zn alloy with CA or RE addition. Mater. Sci. Eng. A. **645**, 196–204 (2015)
15. M.R. Ghandehari Ferdowsi, M. Mazinani, G.R. Ebrahimi, Effects of hot rolling and inter-stage annealing on the microstructure and texture evolution in a partially homogenized AZ91 magnesium alloy. Mater. Sci. Eng. A. **606**, 214–227 (2014)
16. B. Alili, H. Azzeddine, K. Abib, D. Bradai, Texture evolution in AZ91 alloy after hot rolling and annealing. Trans Nonferrous Metals Soc China. **23**, 2215–2221 (2013)
17. H.Y. Wang, E.B. Zhang, X.L. Nan, L. Zhang, Z.P. Guan, Q.C. Jiang, A comparison of microstructure and mechanical properties of Mg–9Al–1Zn sheets rolled from as-cast, cast-rolling and as-extruded alloys. Mater. Des. **89**, 167–172 (2016)
18. M. Zecevic, I.J. Beyerlein, M. Knezevic, Activity of pyramidal I and II <c+a> slip in Mg alloys as revealed by texture development. J. Mech. Phys. Solids. **111**, 290–307 (2018)
19. A. Khosravani, D.T. Fullwood, B.L. Adams, T.M. Rampton, M.P. Miles, R.K. Mishra, Nucleation and propagation of 10–12 twins in AZ31 magnesium alloy. Acta Mater. **100**, 202–214 (2015)
20. H. Asgari, J.A. Szpunar, A.G. Odeshi, Texture evolution and dynamic mechanical behavior of cast AZ magnesium alloys under high strain rate compressive loading. Mater. Des. **61**, 26–34 (2014)
21. M.R. Barnett, Z. Keshavarz, A.G. Beer, X. Ma, Non-Schmid behaviour during secondary twinning in a polycrystalline magnesium alloy. Acta Mater. **56**, 5–15 (2008)
22. M. Wang, L. Luc, C. Li, X.H. Xiao, X.M. Zhou, J. Zhu, S.N. Luo, Deformation and spallation of a magnesium alloy under high strain rate loading. Mater. Sci. Eng. A. **661**, 126–131 (2016)
23. S.G. Hong, S.H. Park, C.S. Lee, Role of 10–12 twinning characteristics in the deformation behavior of a polycrystalline magnesium alloy. Acta Mater. **58**, 5873–5885 (2010)
24. J.H. Lee, S.H. Park, S.G. Hong, J.W. Won, C.S. Lee, Abnormal texture evolution of rolled Mg–3Al–1Zn alloy containing initial 10–12 twins. Scripta Mater. **99**, 21–24 (2015)
25. P. Hidalgo-Manrique, J.D. Robson, M.T. Perez-Prado, Precipitation strengthening and reversed yield stress asymmetry in Mg alloys containing rare-earth elements: a quantitative study. Acta Mater. **124**, 456–467 (2017)
26. L. Capolungo, I.J. Beyerlein, Nucleation and stability of twins in hcp metals. Phys. Rev. B. **78**, 711–729 (2008)
27. J. Jain, W.J. Poole, C.W. Sinclair, M.A. Gharghouri, Reducing the tension–compression yield asymmetry in a Mg–8Al–0.5Zn alloy via precipitation. Scripta Mater. **62**, 301–304 (2010)
28. I.J. Beyerlein, L. Capolungo, P.E. Marshall, R.J. McCabe, C.N. Tome, Statistical analyses of deformation twinning in magnesium. Phil. Mag. **90**, 2161–2190 (2010)
29. J.J. Jonas, S. Mu, T. Al-Samman, G. Gottstein, L. Jiang, E. Martin, The role of strain accommodation during the variant selection of primary twins in magnesium. Acta Mater. **59**, 2046–2056 (2011)
30. H. Yu, Y. Xin, A. Chapuis, X. Huang, R. Xin, Q. Liu, The different effects of twin boundary and grain boundary on reducing tension-compression yield asymmetry of Mg alloys. Sci. Rep. **6**, 29283 (2016)
31. S. Niknejad, S. Esmaeili, N.Y. Zhou, The role of double twinning on transgranular fracture in magnesium AZ61 in a localized stress field. Acta Mater. **102**, 1–16 (2016)

32. A. Levinson, R.K. Mishra, R.D. Doherty, S.R. Kalidindi, Influence of deformation twinning on static annealing of AZ31 Mg alloy. Acta Mater. **61**, 5966–5978 (2013)
33. J.F. Nie, Y.M. Zhu, J.Z. Liu, X.Y. Fang, Periodic segregation of solute atoms in fully coherent twin boundaries. Science. **340**, 957–960 (2013)
34. N. Tahreen, D.L. Chen, M. Nouri, D.Y. Li, Influence of aluminum content on twinning and texture development of cast Mg–Al–Zn alloy during compression. J. Alloys Compd. **623**, 15–23 (2015)
35. M. Ghazisaeidi, L.G. Hector, W.A. Curtin, Solute strengthening of twinning dislocations in Mg alloys. Acta Mater. **80**, 278–287 (2014)
36. F. Guo, D. Zhang, H. Wu, L. Jiang, F. Pan, The role of Al content on deformation behavior and related texture evolution during hot rolling of Mg–Al–Zn alloys. J. Alloy. Compd. **695**, 396–403 (2017)
37. M. Knezevic, A. Levinson, R. Harris, R.K. Mishra, R.D. Doherty, S.R. Kalidindi, Deformation twinning in AZ31: influence on strain hardening and texture evolution. Acta Mater. **58**, 6230–6242 (2010)
38. L. Jiang, J.J. Jonas, A.A. Luo, A.K. Sachdev, S. Godet, Influence of 10–12 extension twinning on the flow behavior of AZ31 Mg alloy. Mater. Sci. Eng. A. **445–446**, 302–309 (2007)
39. X. Gong, S.B. Kang, J.H. Cho, S. Li, Effect of annealing on microstructure and mechanical properties of ZK60 magnesium alloy sheets processed by twin-roll cast and differential speed rolling. Mater Charact. **97**, 183–188 (2014)
40. X. Gong, H. Li, S.B. Kang, J.H. Cho, S. Li, Microstructure and mechanical properties of twin-roll cast Mg–4.5Al–1.0Zn sheets processed by differential speed rolling. Mater. Des. **31**, 1581–1587 (2010)
41. D. Luo, H.Y. Wang, L.G. Zhao, C. Wang, G.J. Liu, Y. Liu, Q.C. Jiang, Effect of differential speed rolling on the room and elevated temperature tensile properties of rolled AZ31 Mg alloy sheets. Mater Charact. **124**, 223–228 (2017)
42. L.L. Chang, J.H. Cho, S.B. Kang, Microstructure and mechanical properties of AM31 magnesium alloys processed by differential speed rolling. J. Mater. Process. Technol. **211**, 1527–1533 (2011)